Regulation of clathrin coat assembly by Eps15 homology domain–mediated interactions during endocytosis

Ryohei Suzuki[a,*], Junko Y. Toshima[a,b,*], and Jiro Toshima[a,b]
[a]Department of Biological Science and Technology, Tokyo University of Science, 2641 Yamazaki, Noda, Chiba 278-8510, Japan; [b]Research Center for RNA Science, Research Organization for Information Science and Technology, Tokyo University of Science, 2641 Yamazaki, Noda, Chiba 278-8510, Japan

ABSTRACT **Clathrin-mediated endocytosis involves a coordinated series of molecular events regulated by interactions among a variety of proteins and lipids through specific domains. One such domain is the Eps15 homology (EH) domain, a highly conserved protein–protein interaction domain present in a number of proteins distributed from yeast to mammals. Several lines of evidence suggest that the yeast EH domain–containing proteins Pan1p, End3p, and Ede1p play important roles during endocytosis. Although genetic and cell-biological studies of these proteins suggested a role for the EH domains in clathrin-mediated endocytosis, it was unclear how they regulate clathrin coat assembly. To explore the role of the EH domain in yeast endocytosis, we mutated those of Pan1p, End3p, or Ede1p, respectively, and examined the effects of single, double, or triple mutation on clathrin coat assembly. We found that mutations of the EH domain caused a defect of cargo internalization and a delay of clathrin coat assembly but had no effect on assembly of the actin patch. We also demonstrated functional redundancy among the EH domains of Pan1p, End3p, and Ede1p for endocytosis. Of interest, the dynamics of several endocytic proteins were differentially affected by various EH domain mutations, suggesting functional diversity of each EH domain.**

Monitoring Editor
David G. Drubin
University of California, Berkeley

Received: May 2, 2011
Revised: Nov 30, 2011
Accepted: Dec 12, 2011

INTRODUCTION

Clathrin-mediated endocytosis is a coordinated series of molecular events, including cargo loading, formation and invagination of coated pits, and vesicle formation (Geli and Riezman, 1998; Engqvist-Goldstein and Drubin, 2003; Sorkin, 2004; Toret and Drubin, 2006). Recent live-cell imaging studies revealed the detailed timing of protein recruitment to sites of clathrin-mediated endocytosis in budding yeast and mammalian cells (Merrifield *et al.*, 2002; Kaksonen *et al.*, 2003, 2005; Ehrlich *et al.*, 2004; Newpher *et al.*, 2005). In yeast, Syp1p, a SGIP1-α–related protein, and Ede1p, a Eps15-related protein, are the earliest proteins known to arrive at sites of endocytosis (Kaksonen *et al.*, 2005; Toshima *et al.*, 2006; Stimpson *et al.*, 2009). Clathrin is also considered to be part of the early coat module, but the precise timing of its recruitment at sites of endocytosis has not been determined because a large proportion of clathrin is localized to highly dynamic intracellular compartments, including the *trans*-Golgi network, and its cortical localization is masked by a strong internal signal (Kaksonen *et al.*, 2005; Newpher *et al.*, 2005). Ent1/2p and Yap1801/2p, which are related to the mammalian clathrin adaptors epsin and AP180/CALM, respectively, have both clathrin- and phosphatidylinositol 4,5-bisphosphate–binding domains and may function to recruit clathrin to sites of endocytosis (Wendland and Emr, 1998; Wendland *et al.*, 1999; Newpher *et al.*, 2005). One to two minutes after Syp1p and Ede1p arrive at such sites, the late coat module, including the Pan1p complex, appears and couples coat formation to actin polymerization in cooperation with Las17p, a yeast WASP, and Myo5p (Kaksonen *et al.*, 2003; Sun *et al.*, 2006).

These coordinated endocytic events are regulated by interactions among a variety of proteins and lipids through specific domains (Engqvist-Goldstein and Drubin, 2003). One such domain is the Eps15 homology domain (EH domain), which is an evolutionarily conserved protein–protein interaction domain present in a number of proteins distributed from yeast to mammals (Di Fiore *et al.*, 1997;

This article was published online ahead of print in MBoC in Press (http://www.molbiolcell.org/cgi/doi/10.1091/mbc.E11-04-0380) on December 21, 2011.

*These authors contributed equally to this work.

Address correspondence to: Jiro Toshima (jtosiscb@rs.noda.tus.ac.jp).

Abbreviations used: EH domain, Eps15 homology domain; mRFP, monomeric red fluorescent protein.

Santolini *et al.*, 1999). The EH domain was originally identified as a domain comprising repeats of ~100 amino acids in the N-terminal region of Eps15, which is a binding partner of α-adaptin, a component of the AP-2 complex and part of the clathrin-coated pit (Benmerah *et al.*, 1995, 1996; van Delft *et al.*, 1997). Several experiments, including phage-display screens and screening of a human fibroblast expression library, demonstrated that the EH domain binds to peptides containing the Asn-Pro-Phe (NPF) sequence (Salcini *et al.*, 1997; Paoluzi *et al.*, 1998). Structural analyses demonstrated that NPF residues are almost completely embedded in a conserved hydrophobic pocket within the EH domain, allowing close contact between the asparagine residue of the tripeptide and a highly conserved tryptophan residue in the EH domain (de Beer *et al.*, 1998, 2000). Mutation of this conserved tryptophan residue dramatically impairs binding of the EH domains to NPF motifs, and the mechanism of EH domain/NPF motif interaction is likely conserved among most EH domains (Salcini *et al.*, 1997; de Beer *et al.*, 1998; Grant and Caplan, 2008).

In yeast, three EH domain–containing proteins (EHDPs)—Pan1p, End3p and Ede1p—have been reported to play important roles during endocytosis. Pan1p is another yeast Eps15-related protein. It contains two EH domains and forms a stable complex with End3p, which also has two EH domains (Raths *et al.*, 1993; Benedetti *et al.*, 1994; Tang *et al.*, 1997; Wendland and Emr, 1998; Toshima *et al.*, 2007). Previous studies showed that Pan1p and Ede1p bind to NPF motifs of the clathrin adaptors Yap1801/2p and/or Ent1/2p and that the dynamics of Pan1p and Ede1p depends on these interactions (Wendland and Emr, 1998; Howard *et al.*, 2002; Aguilar *et al.*, 2003; Maldonado-Baez *et al.*, 2008). These observations suggest that the EH domain/NPF interaction between Eps15-related proteins and clathrin adaptors is conserved from yeast to mammals. Although genetic and cell-biological studies of EHDPs suggest a role for the EH domain in clathrin-mediated endocytosis, functional differences among the EH domains of Pan1p, End3p, and Ede1p and how these EHDPs regulate clathrin coat assembly are not fully understood.

In the present study we find that the EH domains of Pan1p, End3p, and Ede1p function redundantly for efficient assembly of the clathrin coat. By live-cell imaging of cortical patch dynamics, we demonstrate that the patch lifetimes of Pan1p, End3p, and Ede1p are increased when their EH domains are mutated. We also demonstrate that mutations of the EH domains cause a defect of cargo internalization and delay assembly of the clathrin coat without affecting assembly of the actin patch. Furthermore, the EH domains of Pan1p, End3p, and Ede1p are required for proper localization of the endocytic coat proteins Sla1p and Yap1801p, suggesting that the EH domains target these proteins to endocytic sites in order to facilitate clathrin coat assembly.

RESULTS

Mutations in the EH domains of Pan1p, End3p, and Ede1p increase their lifetime at cortical patches

Several lines of evidence indicate that the yeast EHDPs Pan1p, End3p and Ede1p play important roles during endocytosis (Miliaras and Wendland, 2004). The EH domain is frequently present as tandem repeats within a single protein (Santolini *et al.*, 1999; Grant and Caplan, 2008), and Pan1p, End3p, and Ede1p contain two or three EH domains, respectively, in their N-terminal regions (Figure 1A). Previous studies showed that mutation of a highly conserved tryptophan residue in the EH domain impairs its ability to bind to the NPF motif (Salcini *et al.*, 1997; de Beer *et al.*, 2000). To explore in detail the role of the EH domain in yeast endocytosis, we mutated all of the conserved tryptophan residues in the EH domains of Pan1p, End3p, or Ede1p to alanine and integrated them into their endogenous loci (termed *pan1*^{EH}, *end3*^{EH}, and *ede1*^{EH}, respectively). Although *pan1*^{EH} and *ede1* ^{EH} cells were viable at both 37 and 39°C, *end3* ^{EH} cells were temperature sensitive for growth at 39°C (Figure 1B). Because the second EH domain of End3p has only limited similarity and it is unclear whether it really functions as an EH domain (Santolini *et al.*, 1999), we created additional mutants that were mutated in only the first or second EH domain of End3p. We found that both of the mutants were temperature sensitive for growth at 39°C (Supplemental Figure S1A), suggesting that the second EH domain might be important for the function of End3p. To examine the effects of EH domain mutation on EHDP dynamics, we tagged Pan1p, End3p, and Ede1p with green fluorescent protein (GFP) and examined the resulting effects. The GFP-tagged EH domain mutants were expressed at similar levels to the wild-type proteins (Supplemental Figure S1B). All of the GFP-tagged mutants were localized to cortical patches (Supplemental Figure S1, C–E), suggesting that the EH domain/NPF motif interactions are unnecessary for primary targeting of the EHDPs to cortical patches. Consistent with previous reports, Pan1-GFP and End3-GFP patches formed at the cell cortex with lifetimes of 26.5 ± 5.5 and 28.6 ± 4.5 s, respectively, culminating in inward movement (Figure 1C; Kaksonen *et al.*, 2005). Pan1^{EH}-GFP and End3^{EH}-GFP patches formed and disappeared with the typical inward movement, but their lifetimes were increased to 34.6 ± 10.5 and 42.4 ± 7.8 s, respectively (Figure 1C). Tracking of individual patches showed that the distance and timing of the inward movement of Pan1^{EH}-GFP or End3^{EH}-GFP patches was almost the same as that of the wild-type proteins but that the time required to reach the maximum fluorescence intensity was increased (Figure 1D and Supplemental Figure S2), suggesting that mutation in EH domains might causes a delay in accumulation of EHDPs to endocytic sites. Ede1p is an early-arriving endocytic protein that appears at the cell cortex before Sla1p and has a lifetime ranging widely from ~30 to 150 s (Figure 1E; Toshima *et al.*, 2006; Stimpson *et al.*, 2009). Similar to Pan1p and End3p patches, Ede1^{EH}-GFP patches had a significantly increased lifetime, and ~34% of them remained stationary at the plasma membrane for >240 s (Figure 1E). The EH domain therefore seems to be important for efficient recruitment of EHDPs to sites of endocytosis.

Dynamics of the Sla1p patch and actin patch in EH domain mutants

We next examined whether the dynamics of the late coat module and actin patch were affected in the EH domain mutants. We used Sla1-GFP and Abp1–monomeric red fluorescent protein (mRFP) as markers to follow the dynamics of the late coat module and actin patch, respectively (Kaksonen *et al.*, 2003). First, we measured the mean lifetimes of both Sla1-GFP and Abp1-mRFP in each mutant. Of interest, the lifetimes of Sla1-GFP patches were differentially affected by different EH domain mutants. In *pan1*^{EH} cells, Sla1-GFP patches had an average lifetime of 35.9 ± 6.0 s, similar to Sla1-GFP patches in wild-type cells (32.3 ± 5.8 s; Figure 2A). In contrast, the lifetime of Sla1-GFP patches was significantly increased in *end3*^{EH} cells (55.7 ± 17.1 s) and slightly decreased in *ede1*^{EH} cells (25.7 ± 4.1 s; Figure 2A). In contrast, all the mutants showed Abp1-mRFP lifetimes similar to that of wild-type cells (Figure 2A). Next we carried out simultaneous imaging of Sla1p and Abp1p to analyze the dynamic behavior of these proteins in live cells. In wild-type cells, Sla1-GFP was immediately followed by a burst of Abp1-mRFP recruitment, as shown in kymographs generated across a single pixel-wide line of an individual patch (see boxed area in Figure 2B). In all mutants, similar dynamics of Sla1-GFP and Abp1-mRFP patches

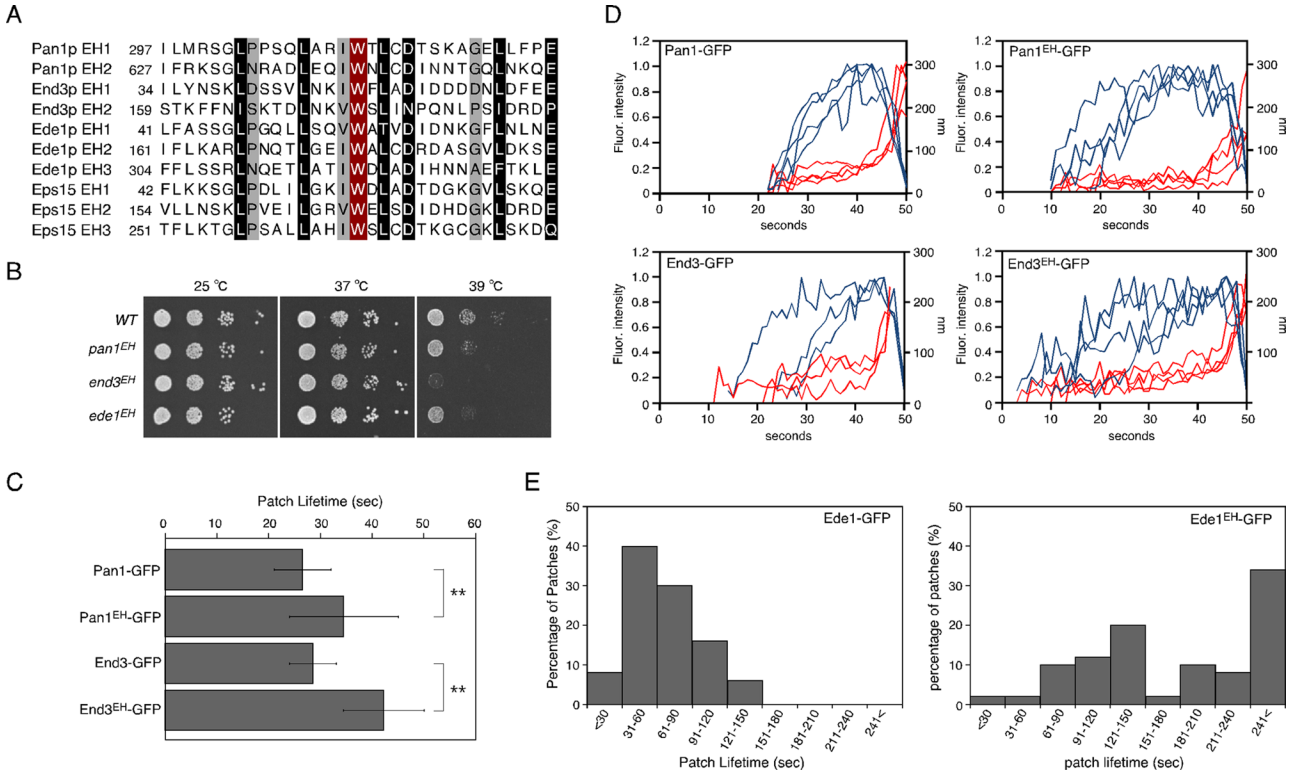

FIGURE 1: Generation and characterization of EH mutants in Pan1p, Ede1p, and End3p. (A) Sequence alignments of the EH domains in Pan1p, End3p, Ede1p, and mouse Eps15. Residues chosen for mutagenesis are highlighted in red. Residues conserved highly and moderately throughout the family are indicated in black and gray, respectively. (B) The *end3*^{EH} mutant was temperature sensitive for growth at 39°C. A dilution series of cells was plated on YPD medium and incubated at 25, 37, or 39°C. (C) Average lifetimes of Pan1-GFP and End3-GFP ± SD in wild-type and mutant cells. Data were taken from 2-min movies with a 1-s frame interval. n = 50 patches for each strain. **$p < 0.001$. (D) Quantification of fluorescence intensity (red) and distance from site of patch formation (blue) as a function of time for patches of indicated GFP-tagged proteins. Each curve represents data from one patch. Behavior of three independent patches was plotted for each strain. (E) Distribution of Ede1-GFP and Ede1^{EH}-GFP patch lifetimes. Movies were taken with a 1-s frame interval. n = 50 patches for each strain.

were observed, except that the time required to reach the maximum fluorescence intensity was increased in *end3*^{EH} mutants or decreased in *ede1*^{EH} mutants (Figure 2B). Taken together, these data indicate that the EH domain is required for regulation of Sla1p coat assembly but not for actin-driven membrane invagination and vesicle internalization.

To clarify whether the NPF-binding pocket is responsible for most of the functions of the EH domain or whether the EH domain has other functionally important interactions, such as lipid binding (Naslavsky *et al.*, 2007), outside the NPF-binding pocket, we deleted the entire EH domains of Pan1p, End3p, and Ede1p (termed *pan1ΔEH*, *end3ΔEH*, and *ede1ΔEH*, respectively) and tested the phenotypic consequences in these mutants. All of the EH deletion mutants were localized to cortical patches, although parts of End3ΔEH-GFP formed a large aggregate in the cytosol, confirming that the EH domains are unnecessary for primary targeting of the EHDPs to cortical patches (Supplemental Figure S3A). The *ede1ΔEH* mutants exhibited almost the same phenotype as the *ede1*^{EH} mutant in terms of growth, localization, and Sla1p and Abp1p dynamics (Supplemental Figure S3, B, D–F). Similar to the *pan1*^{EH} mutant, the *pan1ΔEH* mutant also showed no marked phenotype, except that lifetimes of Pan1p and Sla1p were slightly decreased compared with wild-type cell (Supplemental Figure S3, B, D–F). The NPF-binding pocket therefore seems to be responsible for the major EH domain functions in Pan1p and Ede1p. In contrast, in comparison to the *end3*^{EH} mutant, the *end3ΔEH* mutant exhibited much more severe phenotypic features, which resembled those of the *end3*-null mutant shown previously (Supplemental Figure S3, D–F; Kaksonen *et al.*, 2005). Although Pan1p and Ede1p are relatively large proteins composed of 1480 and 1381 amino acids, respectively, and contain several domain structures, End3p is a small protein (349 amino acids) in which more than half of the structure is occupied by the EH domains. Thus the function of End3p besides the EH domain might be disrupted in the *end3ΔEH* mutant because of structural instability. In addition to the *end3ΔEH* mutant, we also examined the phenotype of another *end3* mutant, *end3 K47E/172E*, in which two lysine residues that are potential sites for lipid binding (Naslavsky *et al.*, 2007) are mutated. The *end3 K47E/172E* mutant exhibited almost the same phenotype as wild-type cells (Supplemental Figure S3, B and E–G), indicating that these sites are not critical for the function of End3.

Functional redundancy of EH domains for endocytic patch formation

To investigate functional redundancy among EHDPs, we analyzed the effect of double or triple mutants on the dynamics of Sla1p or Abp1p. Although *pan1*^{EH} *end3*^{EH} cells were temperature sensitive for growth at 37°C, the growth of *pan1*^{EH} *ede1*^{EH} cells was almost

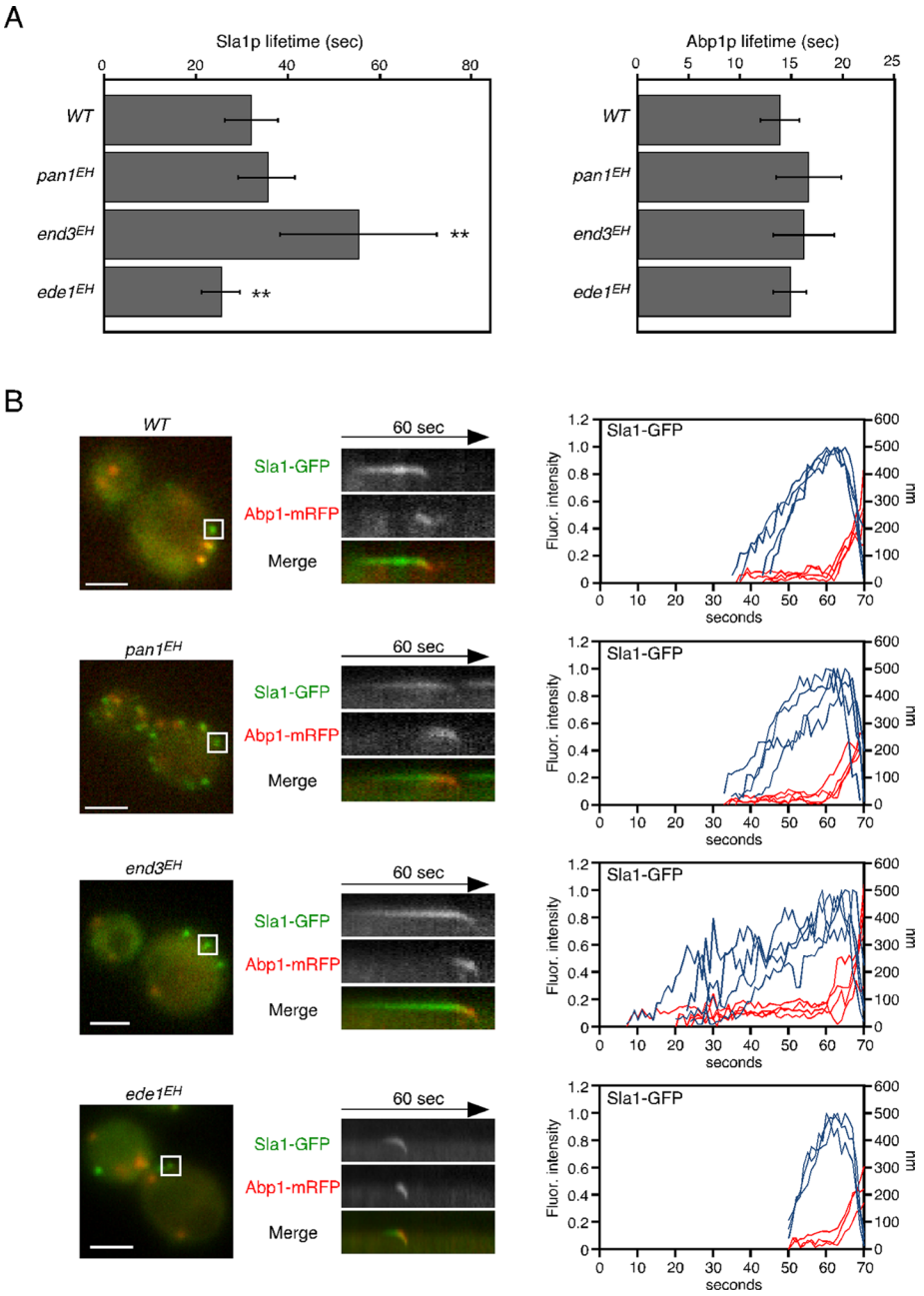

FIGURE 2: Dynamics of the Sla1p patch and actin patch in EH domain mutants. (A) Average lifetimes of Sla1-GFP (left) and Abp1-mRFP (right) ± SD for indicated strains. Data were taken from 2-min movies with a 1-s frame interval. n = 50 patches for each strain. **p < 0.001. (B) Left, localizations of Sla1-GFP and Abp1-mRFP in live cells. Middle, kymograph representations of Sla1-GFP and Abp1-mRFP from the boxed area of strains as indicated. Right, quantification of fluorescence intensity (blue) and distance from the site of patch formation (red) as a function of time for patches of Sla1-GFP. Each curve represents data from one patch. Behavior of three independent patches was plotted for each strain. All movies were taken with a 1-s frame interval for both Sla1-GFP and Abp1-mRFP. The data in A were imaged as single-color movies using optimal GFP filter sets, whereas those in B were imaged as two-color simultaneous movies using narrow band-pass filter sets to completely separate GFP and mRFP fluorescence. Scale bars, 2 μm.

the same as that of wild-type cells (Figure 3A). In addition, the lifetime of Sla1p patches was markedly increased in *pan1*^{EH} *end3*^{EH} cells, whereas the lifetime of Abp1p patches was little affected (Figure 3B). Because *pan1*^{EH} cells have no apparent defects in growth or Sla1p patch lifetime, the function of the EH domains of Pan1p is probably substituted by those of End3p. It is intriguing that the lifetimes of Sla1p patches were decreased in double mutants, including the *ede1*^{EH} mutation, even in *end3*^{EH} cells, which showed a markedly increased Sla1p lifetime (Figures 2A and 3B), indicating that the EH domains of Ede1p have a dominant function in determining the lifetime of Sla1p patches. As shown in kymographs and particle-tracking analysis, inward movement of Sla1p appeared to be normal, but the times required to reach the maximum fluorescence intensity were changed in these double or triple mutants, similar to single mutants (Figure 3C).

We next examined the dynamics of nonmutated Pan1p, End3p, and Ede1p in cells expressing mutant forms of the other EHDPs. Of interest, the dynamics of Pan1p and End3p were quite similar to those of Sla1p: the Pan1p and End3p patch lifetimes were increased in the *end3*^{EH} or *pan1*^{EH} mutants and decreased in the *ede1*^{EH}mutant (Figure 4, A–D). This suggests that Pan1p and End3p are able to form a complex with Sla1p, components of the late endocytic coat module, and act together as reported previously (Tang *et al.*, 2000), even though the functions of the EH domains are disrupted. Ede1p patch lifetimes were increased in all of the *pan1*^{EH}, *end3*^{EH}, and *pan1*^{EH} *end3*^{EH} mutants (Figure 4, E and F).

We further examined the effect on endocytic internalization by assessing the internalization of ^{35}S-labeled α-factor. *end3*^{EH} cells exhibited a modest defect of α-factor internalization, whereas *pan1*^{EH} or *ede1*^{EH} cells had only a slight defect (Figure 5A), consistent with the finding that *end3*^{EH} cells had a more severe phenotype in terms of growth and Sla1-GFP dynamics (Figures 1B and 2A). The relative α-factor internalization rates of the mutants are compared in the histogram shown in Figure 5B. Unexpectedly, combination of the *end3*^{EH} and *pan1*^{EH} mutations had no additive effect, although they exhibited a synthetic growth defect (Figures 3A and 5B). The *end3*^{EH} mutant also had little additive effect on α-factor internalization when combined with *ede1*^{EH} cells but a remarkable effect when combined with *pan1*^{EH} *ede1*^{EH} cells (triple mutant; Figure 5B). This result suggested that *pan1*^{EH} and *ede1*^{EH} cells exhibited a redundant function only when combined with *end3*^{EH} cells. These results clearly demonstrate the presence of functional redundancy among these three EHDPs.

Dynamics of the early endocytic component in EH domain mutants

Similar to mammalian cells, clathrin in yeast is localized to cortical patches (Merrifield *et al.*, 2002; Kaksonen *et al.*, 2003, 2005;

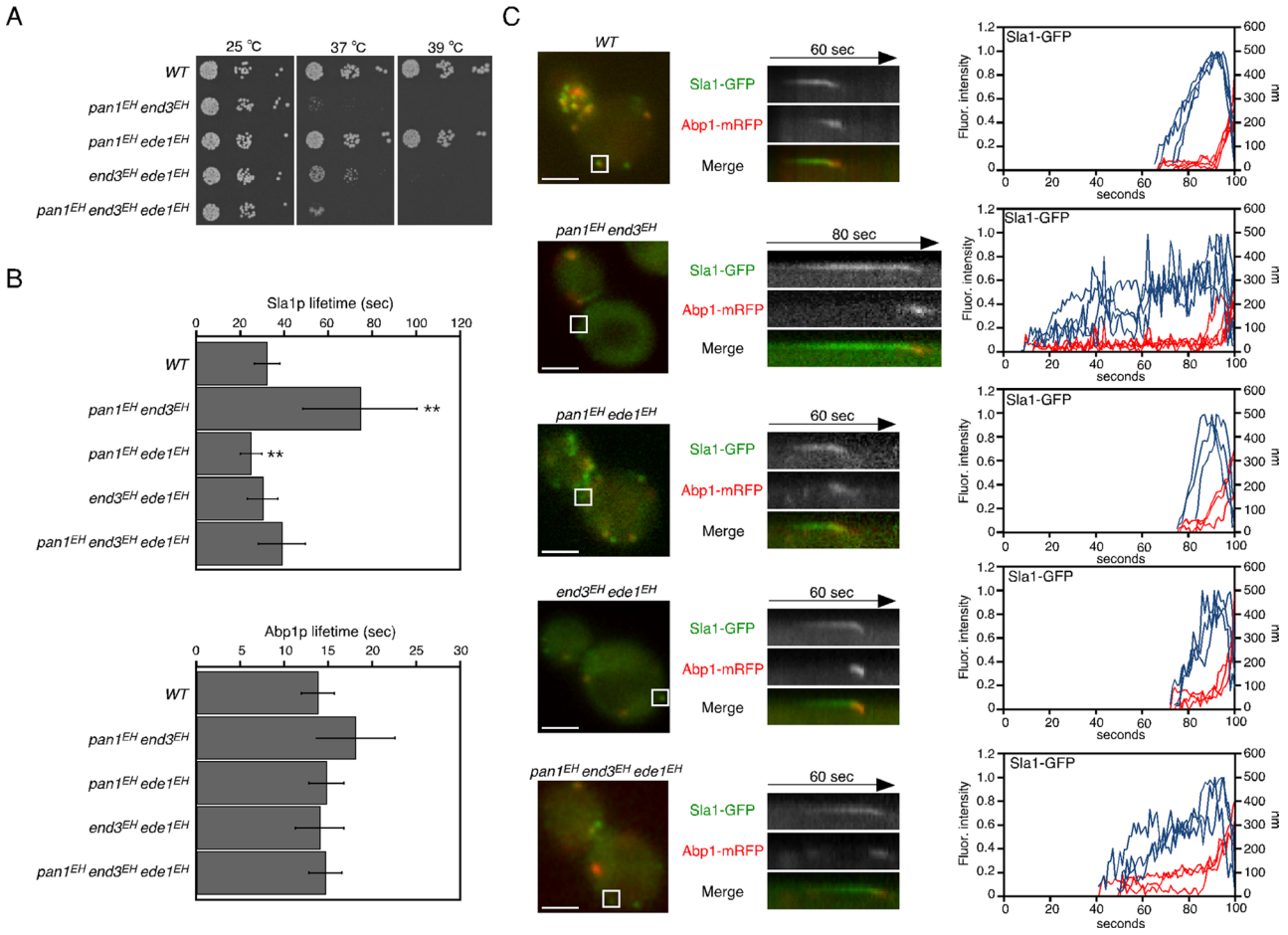

FIGURE 3: Redundant function of EH mutants in endocytic patch formation. (A) The *pan1*^{EH} *end3*^{EH} and triple mutants were temperature sensitive for growth at 37°C. A dilution series of cells was plated on YPD medium and incubated at the indicated temperature. (B) Patch lifetimes of Sla1-GFP (top) and Abp1-mRFP (bottom) ± SD in the indicated strains. Data were obtained from 2-min movies taken with a 1-s frame interval. n = 50 patches for each strain. **p < 0.001. (C) Left, localization of Sla1-GFP and Abp1-mRFP from the strains indicated. Middle, kymograph representations of Sla1-GFP and Abp1-mRFP from the boxed area for the indicated times. Right, quantification of fluorescence intensity (blue) and distance from site of patch formation (red) as a function of time for patches of Sla1-GFP. Each curve represents data from one patch. Behavior of three independent patches was plotted for each strain. All movies were taken with a 1-s frame interval for both Sla1-GFP and Abp1-mRFP. Scale bars, 2 μm.

Newpher *et al.*, 2005). Clathrin appears early at all sites of endocytosis, preceding Sla1p, and has a mean lifetime of ~73.8 s (Kaksonen *et al.*, 2005; Newpher *et al.*, 2005). Therefore we next examined whether the overall process of clathrin coat assembly was affected by EH domain mutations. Because a large proportion of clathrin localizes to intracellular compartments, such as the *trans*-Golgi network, in addition to cortical patches and it is difficult to analyze the cortical localization precisely (Kaksonen *et al.*, 2005; Newpher and Lemmon, 2006), we used another early-arriving endocytic protein, Syp1p, which has a long and variable lifetime similar to that of clathrin, as a marker of clathrin-coat assembly (Stimpson *et al.*, 2009). To analyze extremely long lifetimes of Syp1p in the EH mutants (Figure 6), we tagged Syp1p with three tandem tagged copies of GFP (3GFP). The 3GFP-tagged Syp1p showed similar localization to Syp1-GFP at the cortical patches in addition to the bud neck, as reported previously (Supplemental Figure S4, A and B; Stimpson *et al.*, 2009). The lifetime of Syp1p patches labeled by Syp1-3GFP in wild-type cells ranged from 50 to 350 s, with an average of 118.1 ± 51.0 s (Figure 6, A and C). The lifetime of Syp1-3GFP patches was a little longer compared with that of single GFP–tagged Syp1p (Stimpson *et al.*, 2009) because of the enhanced fluorescence (Supplemental Figure S4C). All single mutants showed increased Syp1p patch lifetimes relative to wild-type cells, even in *ede1*^{EH} cells (Figure 6, A and C, and Supplemental Figure S4D). These effects were enhanced modestly in the *pan1*^{EH} *end3*^{EH} double mutant and clearly in the triple mutant (Figure 6, B and C). For other double mutations, such as *pan1*^{EH} *ede1*^{EH} or *end3*^{EH} *ede1*^{EH}, no additive effect was observed (Figure 6C). It was noteworthy that these results were well consistent with those of α-factor internalization, shown in Figure 5B. Kymographs for these mutants showed that majority of Syp1p patches had extended lifetimes but regularly disappeared from the cell cortex in all mutants (Figure 6D).

To determine the precise timing of Syp1p and Sla1p recruitment to the cortical patches, we imaged the cells expressing Syp1-3GFP and Sla1-mCherry. In wild-type cells, Syp1p appeared ~61.4 s prior to Sla1p and stayed with Sla1p for ~28.9 s at the cortical patch (Figure 7, A and B). Mutations in the EH domains of Pan1p caused the lifetime of Syp1p to increase but had almost no effect on the lifetimes of Sla1p and Abp1p (Figure 2A and 6B). In agreement with these results, in the *pan1*^{EH} mutant, only the timing of Sla1p recruitment

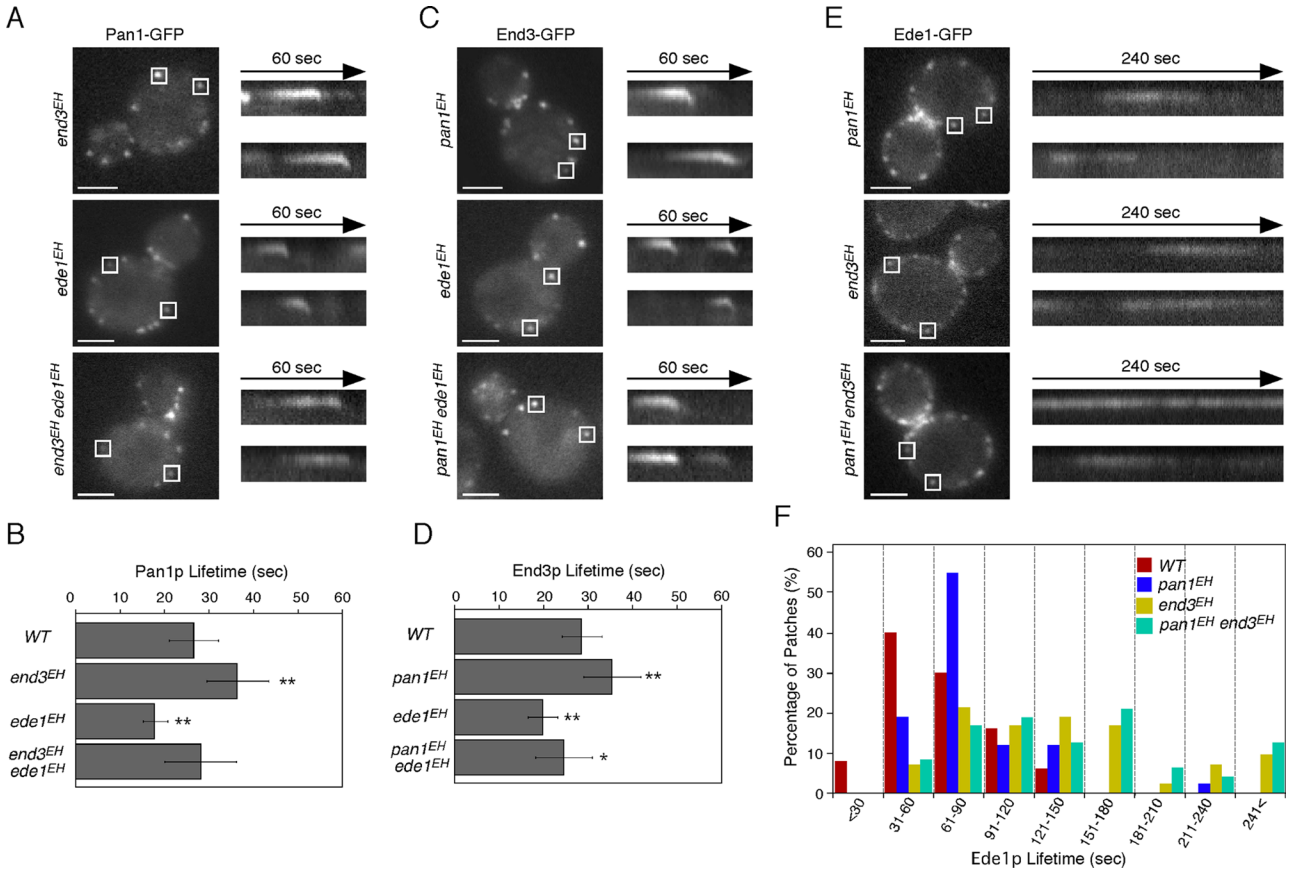

FIGURE 4: Localization of EH domain proteins in EH domain mutants. (A, C, E) Localization of Pan1-GFP (A), End3-GFP (C), and Ede1-GFP (E) in cells expressing mutant forms of other EH domain proteins. Right, kymographs from the same movies. (B, D) Average lifetimes of Pan1-GFP and End3-GFP ± SD in mutant cells. Data were taken from 2-min movies with a 1-s frame interval. n = 50 patches for each strain. *p < 0.01, **p < 0.001. Scale bars, 2 μm. (F) Distribution of Ede1-GFP patch lifetimes in wild-type and indicated mutant cells. n = 50 patches for each strain. Movies were taken with a 1-s frame interval.

after the appearance of Syp1p at the cortical patch was delayed (Figure 7, A and B). Mutations in the EH domains of End3p caused an increment of the lifetimes of both Syp1p and Sla1p (Figure 2A and 6B) and, as a result, delayed the recruitment of Sla1p and extended the time of colocalization between Syp1p and Sla1p (Figure 7, A and B). In the *ede1*^{EH} mutant, the lifetime of Syp1p patches was increased but that of Sla1p patches was decreased (Figure 2A and 6B), resulting in a significant delay of Sla1p recruitment and a decreased colocalization time (Figure 7, A and B). It follows from these results that assembly of the late coat module marked by Sla1p is delayed during endocytosis in all EH mutants, especially the *end3*^{EH} and *ede1*^{EH} mutants.

The frequency of endocytic internalization is decreased in the triple mutant

To examine whether Syp1p patches, which have extended lifetimes in the triple mutants, are eventually internalized or disappear without internalization, we coexpressed Syp1-3GFP and Abp1-mRFP and examined their localization on the cell surface. In wild-type cells, most of the Syp1-3GFP patches were joined by Abp1-mRFP and then disappeared (99.2%, n = 129; Figure 8, A and B). Similarly, it was observed that most Syp1-3GFP patches, despite having greatly extended lifetimes (>300 s) in the triple mutant, became colocalized with Abp1-mRFP for a short time and then disappeared (96.1%, n = 129; Figure 8, A and B). This observation indicates that most of the Syp1-3GFP–labeled endocytic sites in the triple mutants are capable of being internalized into the cytosol.

Having previously reported that *ede1*Δ mutants form fewer Sla1p-labeled endocytic sites than wild-type cells (Stimpson *et al.*, 2009), we assessed the number of endocytic sites in the triple mutants. Maximum-intensity Z projections of live cells were analyzed to determine the average number of patches per surface area. Patch densities were quantified only in the mother cells, in which individual patches were distinguishable. As shown in Figure 8C, in the triple mutant, there was no decrease in the number of Syp1p patches per surface area relative to wild-type cells. We further examined whether EH domain mutations could affect the frequency of endocytotic internalization by comparing the number of Abp1-mRFP patches—a marker of actin-driven membrane invagination and endocytotic vesicle internalization. Maximum-intensity projections of Z stacks revealed that the number of endocytotic internalizations labeled with Abp1-mRFP decreased by ~41% in the triple mutants (Figure 8D). This observation suggests that the frequency of endocytotic internalization is decreased in the triple mutants and that this might cause a reduction of α-factor internalization.

Effects of EH domain mutants on proteins containing the NPF motif

Having established that EH domains interact with NPF motifs (Salcini *et al.*, 1997; de Beer *et al.*, 1998; Paoluzi *et al.*, 1998), we next

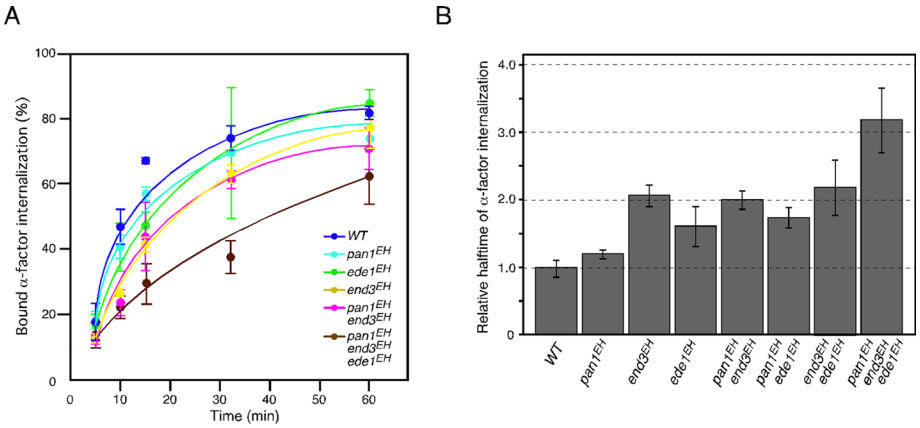

FIGURE 5: Effects of EH mutations on endocytic internalization. (A) Radiolabeled α-factor internalization assays performed on cells expressing the indicated strains at 25°C. Each curve represents the average of three independent experiments, and error bars indicate the SD at each time point. (B) A histogram representing the relative half-time of the α-factor internalization rate calculated from an exponential curve fit on the assay shown in A. Error bars indicate the SD from at least three experiments.

examined whether EH domain mutations could affect the localization or dynamics of NPF motif–containing proteins. Ent1p and Ent2p, an essential pair of genes belonging to the epsin family (Chen *et al.*, 1998; Wendland *et al.*, 1999; Aguilar *et al.*, 2003), contain two NPF motifs that interact with the EH domains of Pan1p and Ede1p (Aguilar *et al.*, 2003). To evaluate precisely differences in the localization of NPF-containing proteins, we compared the triple mutants expressing Ent1-GFP or Ent2-GFP directly alongside wild-type cells (Figure 9A). To distinguish the wild-type and mutant cells, we treated the former with the vacuolar dye 3-triethylammoniumpropyl-4-*p*-diethylaminophenylhexatrienyl pyridinium dibromide (FM4-64). As shown in Figure 9, A and B, the fluorescence intensity of individual Ent1p or Ent2p patches was little affected, indicating that recruitment of these proteins was not dependent on the EH domains. In contrast, the lifetimes of Ent1p patches and Ent2p patches were affected differently by the EH domain mutants: Ent2p patches had a lifetime ~2.5-fold longer in the triple mutants (64.0 ± 19.0 s) than in the wild-type cells (25.4 ± 4.4 s), whereas the Ent1p patch lifetime was extended only modestly (Figure 9C). We also examined the corresponding effect on two other NPF motif-containing proteins, Yap1801p and Yap1802p, which are homologues of the mammalian clathrin adaptor proteins CALM/AP180 (Wendland and Emr, 1998). Yap1802-GFP patches in the triple mutant also showed no marked change in fluorescence intensity but had a slightly extended lifetime relative to those in wild-type cells (Figure 9, A–C). In contrast to these proteins, however, the fluorescence intensity and lifetime of Yap1801-GFP were markedly decreased in the triple mutants (Figure 9, A–C). These results prompted us to examine other endocytic coat proteins, such as Sla1p and Sla2p. We found that Sla2-GFP patches exhibited a phenotype similar to that of Ent2-GFP patches, whereas the fluorescence intensities of Sla1-GFP patches were decreased in the triple-mutant cells relative to the wild-type cells (Figure 9, A–C). These results suggest that EHDPs seem important for the proper accumulation and dynamics of NPF-containing proteins at an endocytic patch. Because Sla1p contains a single NPF sequence at the C terminus (amino acids 2040–2042), we examined whether this NPF sequence is responsible for Sla1p localization. The GFP-tagged Sla1p$^{NPF\text{-}AAA}$ mutant in which the NPF sequence was converted to three alanine residues showed normal localization and lifetimes in wild-type cells (Supplemental Figure S5A). We also found that Sla1p$^{NPF\text{-}AAA}$-GFP exhibited similar dynamics to wild-type Sla1p in the *end3^{EH}* and *ede1^{EH}* mutants (Supplemental Figure S5B), indicating that the NPF sequence is not required for Sla1p localization.

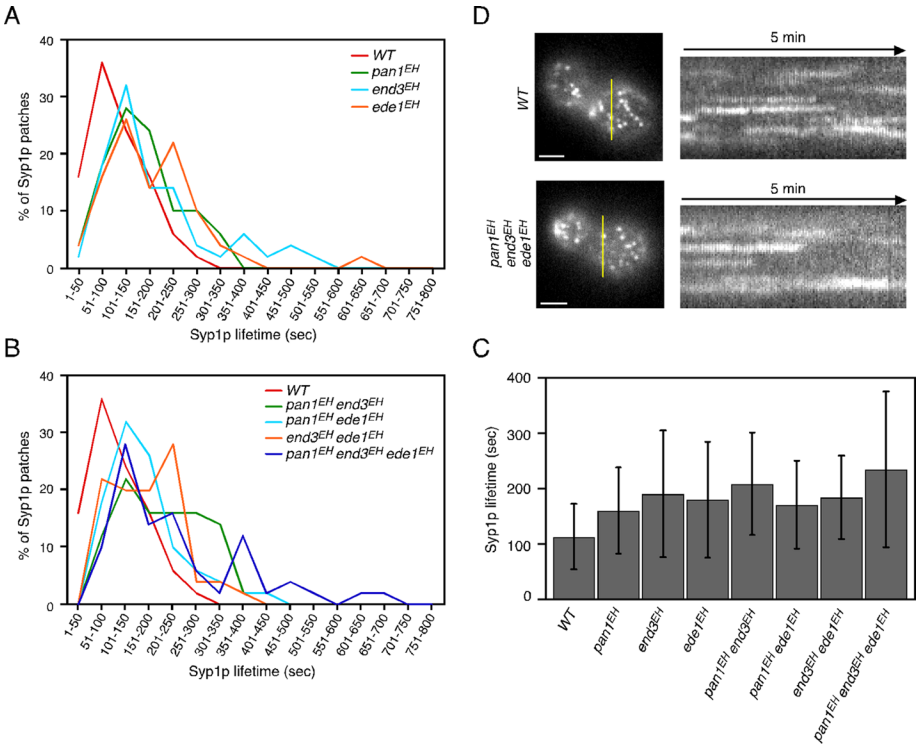

FIGURE 6: Dynamics of Syp1p patch in EH domain mutants. (A, B) Distribution of Syp1p patch lifetimes in the indicated single (A) or double and triple EH domain mutants (B). Data were taken from ~13-min movies with a 4-s frame interval. (C) Average lifetimes of Syp1-GFP ± SD for indicated strains. (D) Left, localization of Syp1-3GFP from the indicated strains. Yellow bars mark where the kymograph was generated. Right, kymograph representations of Syp1-3GFP from 5-min movies. Scale bars, 2 μm.

DISCUSSION

EH domains of End3p, rather than those of Pan1p, play a critical role in endocytosis

In this study we mutated all of the EH domains of yeast endocytic EHDPs—Pan1p, End3p, or Ede1p—and evaluated their effects on several endocytosis-related processes, including recruitment of endocytic

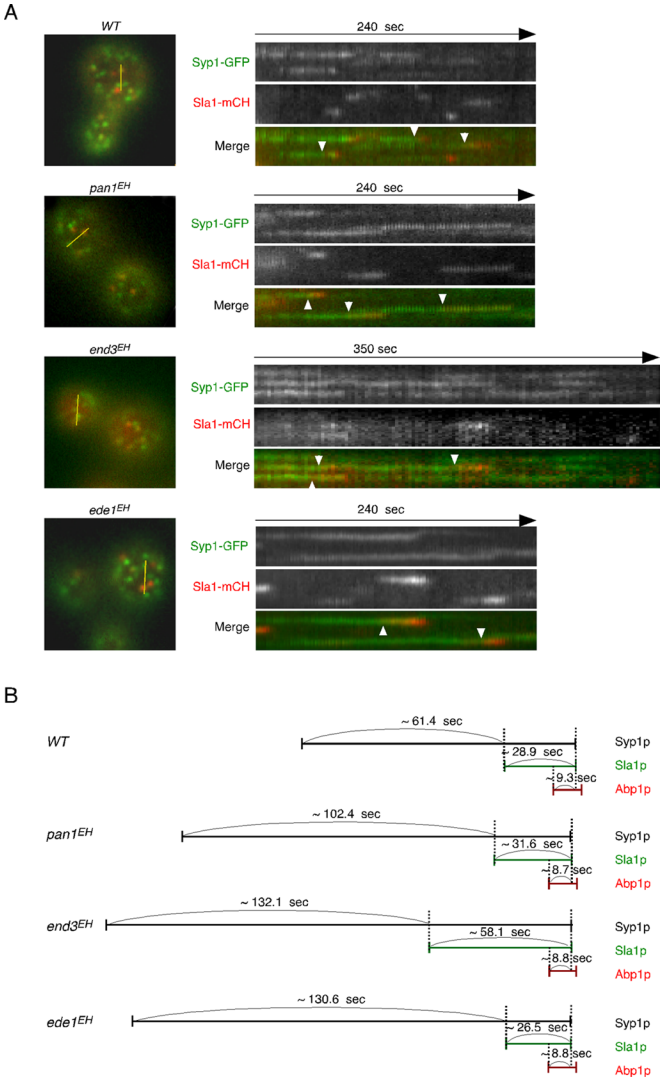

FIGURE 7: Localization and temporal relationship of Syp1p and Sla1p patches in EH domain mutants. (A) Left, localization of Syp1-GFP and Sla1-mCherry (mCH) in live cells. Yellow bars mark where the kymograph was generated. Right, kymograph representations of Syp1-3GFP and Sla1-mCherry from 4- or 6-min movies. Arrowheads indicate examples of Syp1p patches that are joined by Sla1-mCherry. All movies were taken with a 3-s frame interval for both Syp1-GFP and Sla1-mCherry. Scale bars, 2 μm. (B) Temporal relationship of Syp1p, Sla1p, and Abp1p patches in EH domain mutants. Average time was obtained from at least 30 independent patches.

proteins to cortical patches, cargo internalization, and clathrin coat assembly. Previous studies revealed that native Pan1p and End3p form a stable complex with 1:1 stoichiometry (Tang *et al.*, 1997; Toshima *et al.*, 2007) and that therefore these proteins may function as a complex containing four EH domains. Among these EH domains, those of End3p seem to be relatively important since the *end3^{EH}* mutant has more severely defective growth and endocytosis than the *pan1^{EH}* mutant. Unexpectedly, the *pan1^{EH}* mutant exhibited only minor endocytic defects, even though *PAN1* is an essential gene and a variety of *pan1* mutants have been reported to exhibit severe defects of the actin cytoskeleton and/or endocytosis (Tang and Cai, 1996; Tang *et al.*, 2000; Wendland *et al.*, 1996; Toshima *et al.*, 2005). This result differs from a previous observation that the lifetime of Pan1p was significantly extended when its EH domain was mutated (Maldonado-Baez *et al.*, 2008). Maldonado-Baez *et al.* (2008) showed that ~60% of Pan1^{EH}-GFP patches exhibited greatly extended lifetimes ranging from 75 to >120 s, whereas the remaining ~40% had slightly extended lifetimes (45 ± 5 s). The different lifetimes of Pan1^{EH}-GFP patches might be caused by differences in their manner of expression; in their experiment, Pan1^{EH}-GFP was expressed via its endogenous promoter using a single-copy plasmid in *pan1*Δ cells, whereas we expressed Pan1^{EH}-GFP from an endogenous locus. Any defects in the *pan1^{EH}* mutant are probably masked by End3p because they work together as a complex and have redundant functions (Tang *et al.*, 1997; Toshima *et al.*, 2007).

Role of the EH domains of Ede1p in endocytosis

As opposed to the *pan1^{EH}* or *end3^{EH}* mutant, we found a decrease of ~20.5% in the lifetime of the Sla1-GFP patch in the *ede1^{EH}* mutant relative to wild-type cells. This effect is in agreement with earlier observations of Sla1-GFP in *ede1*Δ cells (Kaksonen *et al.*, 2005; Stimpson *et al.*, 2009). Of interest, the *ede1^{EH}* mutant also decreased the lifetime of the Sla1-GFP patch even when combined with the *pan1^{EH}* or *end3^{EH}* mutant. Moreover, prolonged Sla1-GFP patch lifetime observed in *pan1^{EH} end3^{EH}* double mutant (Figure 3, B and C) was reduced when the double mutant was combined with the *ede1^{EH}* mutant. These results suggest that the EH domains of Ede1p have a dominant role in determining the lifetime of the Sla1p patch. Although it has not been clarified how Ede1p regulates Sla1p localization, physical interaction might be important, as the third SH3 domain of Sla1p interacts with Ede1p (Tonikian *et al.*, 2009). In contrast to the Sla1p patch, the lifetimes of the Ede1p and Syp1p patches were increased in *ede1^{EH}* cells, suggesting that the total time required for completion of clathrin coat assembly is increased in the *ede1^{EH}* mutant.

The presence of several phenotypes that are distinct between *ede1^{EH}* and *ede1*Δ cells suggests a specific function of the Ede1p EH domain. For instance, in *ede1*Δ cells, Syp1p was strongly concentrated at the necks of buds, and cortical Syp1p was diffusely and unstably localized with polarization toward the daughter cell (Stimpson *et al.*, 2009), whereas *ede1^{EH}* mutants, as was the case in wild-type cells, exhibited cortical localization of Syp1p but had a lifetime that was increased approximately twofold. Another distinct phenotype was that deletion of the *EDE1* gene reduced the number of endocytic sites (Stimpson *et al.*, 2009), whereas the *ede1^{EH}* mutant had a normal number of Syp1p patches, similar to the triple mutant (data not shown). Thus these observations suggest that the EH domains of Ede1p have a role in efficient assembly of the clathrin-coated pit but not in the regulation of Syp1p localization or endocytic site formation.

EH domains are required for early coat assembly

Although mutation of EH domains caused defects in coat proteins dynamics, no apparent effect was observed in Abp1p, a marker of actin-driven membrane invagination. This result is of interest because mutation of endocytic proteins can often affect the entire process of endocytosis. For instance, deletion of *CHC1*—the clathrin heavy chain—reduces the patch lifetimes of several coat proteins and, in contrast, extends the patch lifetime of Abp1p (Kaksonen *et al.*, 2005; Newpher and Lemmon, 2006). *end3*Δ cells exhibited prolonged patch lifetimes for both coat proteins and Abp1p (Kaksonen *et al.*, 2005). The *pan1-15TA* mutant, in which major potential Prk1p phosphorylation sites in Pan1p are mutated to alanine, exhibited a large abnormal actin structure, including several endocytic proteins (Toshima *et al.*, 2005). Therefore our

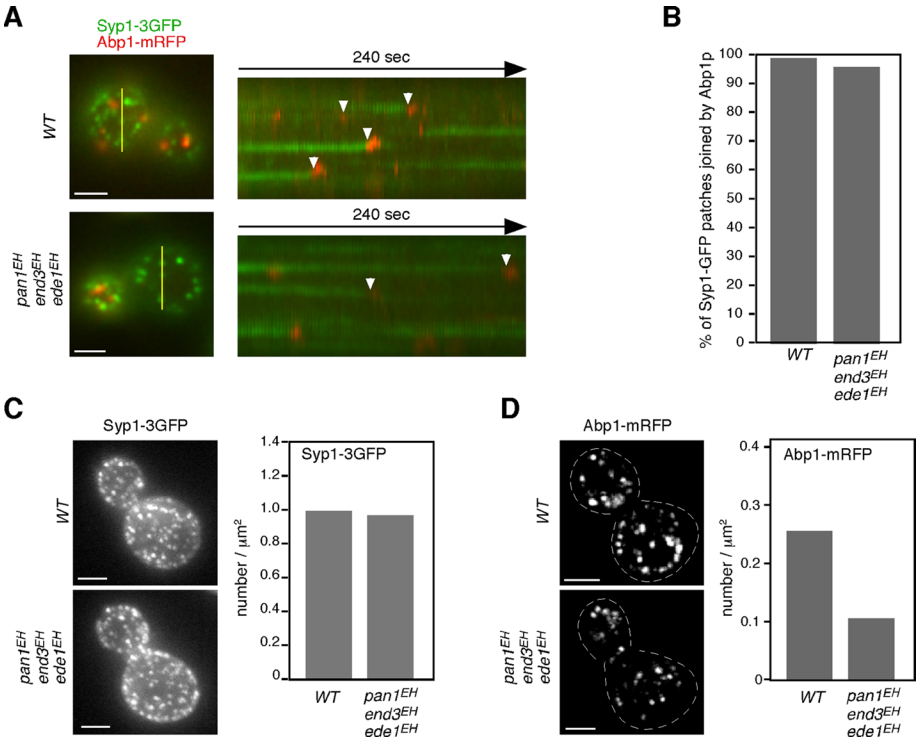

FIGURE 8: All Syp1p patches are eventually internalized in triple mutants. (A) Epifluorescence images of a single cell coexpressing Syp1-3GFP and Abp1-mRFP. Yellow bars mark where the kymograph was generated. Right, kymograph representations of Syp1-3GFP and Abp1-mRFP from 3-min movies. Arrowheads indicate examples of Syp1p patches that are joined by Abp1-mRFP. Scale bars, 2 µm. (B) Percentage of the Syp1-3GFP patches that were eventually joined by Abp1-mRFP. (C, D) Maximum-intensity projections of Z stacks of wild-type and triple-mutant cells labeled with Syp1-3GFP (C) or Abp1-mRFP (D). The Z series was acquired through the entire cell at 0.2-µm intervals. Dotted lines represent outline of cells. Quantification of Syp1-3GFP or actin patches/µm^2 ± SD in wild-type and triple mutant cells (n = 50 cells for each strain). Scale bars, 2 µm.

observation suggests a specific role of EH domain–mediated interactions in the process of early clathrin coat assembly.

How does mutation of EHDPs affect early coat assembly? Because Ede1 was previously characterized as a binding partner of Syp1p (Reider *et al.*, 2009; Stimpson *et al.*, 2009), it seems reasonable to suppose that Syp1p lifetime is increased in *ede1^{EH}* cells because Ede1^{EH} patch lifetime is increased. However, it is still unclear why the lengthened Syp1p lifetime is also observed in the *pan1^{EH}* and *end3^{EH}* mutants. By tracking individual Syp1p patches in the *pan1^{EH}* and *end3^{EH}* mutants, we found that the time required to reach the maximum fluorescence intensity was not increased in these mutants (Supplemental Figure S4D), although Syp1p patch intensities were quite irregular, as reported previously (Stimpson *et al.*, 2009). This observation suggests that early coat assembly might be suspended until recruitment of late coat proteins such as Yap1801p and Sla1p begins. How late coat module determines lifetimes of early coat proteins is an important question for the future.

EH domains are required for Yap1801p recruitment

Among the yeast NPF proteins, only Yap1801p exhibited a decrease of both fluorescence intensity and lifetime at cortical patches in the triple EH domain mutant. Yap1801p is the yeast homologue of AP180/CALM family proteins, which are associated with clathrin assembly activity (Wendland and Emr, 1998). AP180 and CLAM have similar roles in facilitating assembly of the clathrin coat and controlling the size of clathrin-coated vesicles (Ahle and Ungewickell, 1986; Ye *et al.*, 1995; Ye and Lafer, 1995; Morgan *et al.*, 1999; Meyerholz *et al.*, 2005). It is intriguing that Morgan *et al.* (2003) reported that squid Eps15 stimulated clathrin assembly by AP180 via NPF motif/EH domain interaction, although Eps15 itself is not capable of polymerizing clathrin. The role of yeast AP180 proteins was unclear, as deletion of both *YAP180* genes resulted in no apparent defect of endocytosis or growth (Huang *et al.*, 1999), although a recent study showed that NPF motifs in Yap1801/2p and Ent1/2p share a complementary role in both viability and endocytosis (Maldonado-Baez *et al.*, 2008). It is unclear how a decreased level of Yap1801p at cortical patches affects clathrin coat assembly, whereas defective recruitment of some additional factors might cooperatively cause defects. It was reported that some EH domains recognize other peptide motifs, including Phe–Trp (FW), Trp–Trp (WW), and Ser–Trp–Gly (SWG) (Paoluzi *et al.*, 1998). The EH domain of End3p was also shown to interact with peptides containing the His–(Thr/Ser)–Phe (HTF/HSF) motif (Paoluzi *et al.*, 1998). Using the PatMatch (Yeast Genome Pattern Matching) program, we found that the FW sequence(s) exists in Chc1p, yeast clathrin heavy chain, and Apl1p, a large subunit of the clathrin-associated protein complex (AP-2). We also found that two WW sequences are present in Sla1p. These motifs would be attractive targets for further investigation of how EHDPs regulate clathrin-coated pit assembly.

Function of EH domains in endocytosis is conserved in both yeast and mammals

There are several lines of evidence to suggest that mammalian Eps15p has a similar function to yeast EHDPs. First, it was shown that clathrin-coated pit assembly is perturbed by overexpression of the Eps15 mutant lacking the second and third EH domains (Benmerah *et al.*, 1999). A previous study demonstrated that EH domains are required but are not sufficient for targeting Eps15 to clathrin-coated pits (Benmerah *et al.*, 2000). Knockdown of Eps15 increases the lifetime of clathrin, indicating that Eps15 is critical for efficient assembly of the clathrin coat (Mettlen *et al.*, 2009). Thus the role of the EH domain in the endocytic pathway seems to be conserved between yeast and animal cells.

MATERIALS AND METHODS

Yeast strains, growth conditions, and plasmids

The yeast strains used in this study are listed in Table 1. All strains were grown in standard rich medium (yeast extract/peptone/dextrose [YPD]) or synthetic medium supplemented with 2% glucose and appropriate amino acids. *pan1^{EH}*, *end3^{EH}*, or *ede1^{EH}* mutant was integrated as follows: To create a *pan1* integration plasmid, the *Xmn*I–*Dra*I fragment of the *PAN1* gene was cloned into pBluescript II SK (pBS), and the *Sal*I fragment of the *LEU2* gene was inserted into the *Sal*I site 154 base pairs upstream of the *PAN1* open reading frame (ORF). The mutated *Msc*I–*Nhe*I *pan1* fragments were used to replace the *PAN1* gene in the integration plasmid. To integrate

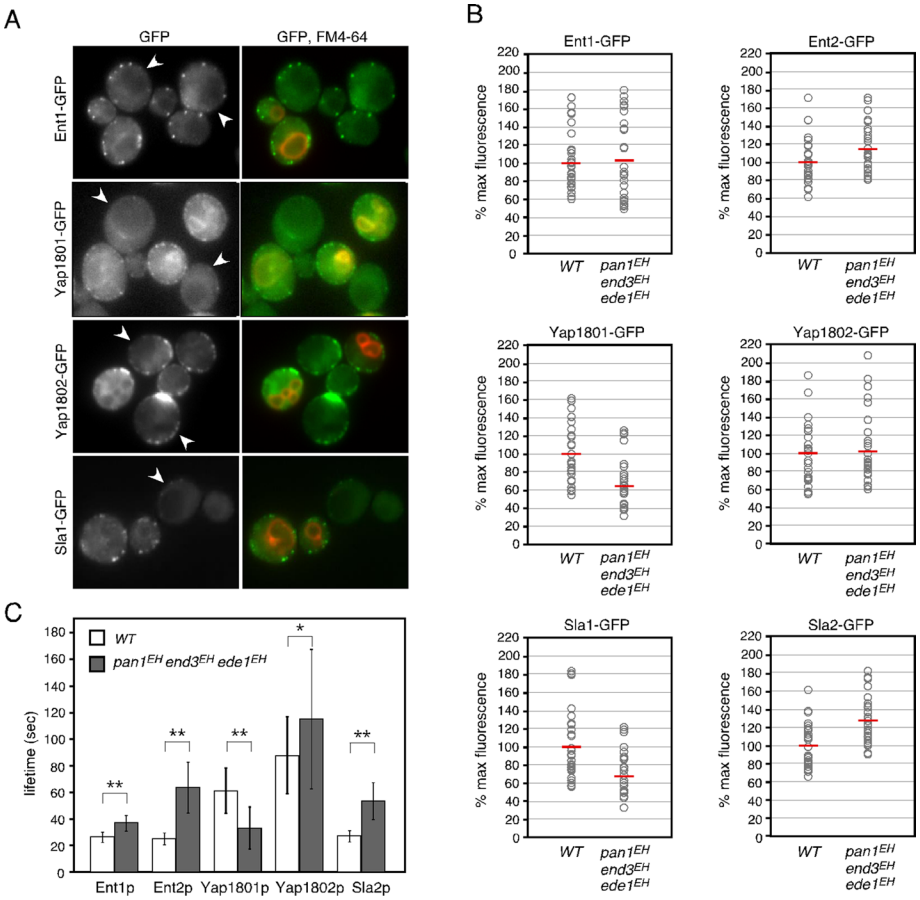

FIGURE 9: Effects of EH domain mutations on endocytic proteins. (A) Localization of GFP-tagged endocytic proteins in wild-type and triple-mutant cells. Two strains were mixed and acquired in the same images. Only wild-type cells were labeled with FM4-64 in the right-hand images. Arrowheads indicate triple mutant cells. (B) The relative maximum fluorescence intensities of indicated GFP-fused proteins at cortical patches. Intensities of individual patches were compared in the same image by mixing wild-type and triple-mutant cells, which were distinguishable from FM4-64-treated wild-type cells. The values of intensities for wild-type and triple-mutant cells were divided by the mean for patch intensities in wild-type cells (n = 30), and the resulting values were multiplied by 100. Each open circle and horizontal red line represents intensity of a single patch and the mean of the intensities, respectively. (C) Patch lifetimes ± SD of GFP-tagged endocytic proteins in wild-type and triple mutant cells. Data were obtained from ~3-min movies taken with a 1-s frame interval. n = 50 patches for each strain. *p < 0.01, **p < 0.001.

pan1^{EH} mutant at the endogenous locus, the integration plasmids were digested with *Sac*I and *Xba*I and transformed into *pan1*Δ::*HIS3/PAN1* diploid strains. Integrated *pan1* mutants were selected on synthetic complete plates lacking leucine and sporulated to obtain *pan1* mutants. To create *end3* integration plasmids, the *Xba*I-*Cla*I fragment of the *END3* gene was cloned into pBS, and the *Sma*I fragment of the *URA3* gene was inserted into the EcoO109I site 150 base pairs upstream of the *END3* ORF. The mutated *Xba*I–*Xho*I *end3* fragments were used to replace the *END3* gene in the integration plasmid. To integrate *end3^{EH}* mutants at the endogenous locus, the integration plasmids were digested with *Xba*I and *Cla*I and transformed into *end3*Δ strains. To create *ede1* integration plasmid, the *Sac*I–*Xho*I fragment of the *EDE1* gene was cloned into pBS, and the *Sma*I fragment of the *LEU2* gene was inserted into the *Eco*RV site, which was made by amino acid substitutions, at 139 base pairs downstream of the *EDE1* ORF. The mutated *Sac*I–*Nde*I *ede1* fragment was used to replace the *EDE1* gene in the integration plasmid. To integrate *ede1^{EH}* mutant at the endogenous locus, the integration plasmids were digested with *Sac*I and *Xho*I and transformed into *ede1*Δ strains. Amino acid substitutions were made using QuikChange XL Site-Directed Mutagenesis Kit (Stratagene, Santa Clara, CA). *pan1ΔEH* mutant was constructed by inserting the PCR-amplified fragment (nucleotides [nt] 1074–1784) into the *PAN1* fragment deleting EH domains and the region between the EH domains (nt 787–2063). Similarly, *end3ΔEH*, or *ede1ΔEH* mutant was constructed by inserting the PCR-amplified fragments (*END3*, nt 289–366; *EDE1*, nt 298–381 and 664–807) into the *END3* or *EDE1* fragment deleting EH domains and the region between the EH domains (*END3*, nt 16–663; *EDE1*, nt 19–1107). GFP and mRFP tags were integrated at the C terminus of each gene (Longtine *et al.*, 1998). The triple-GFP tag was integrated at the C-terminus of the *SYP1* gene as follows: The 3GFP fragment was subcloned into *Bam*HI- and *Not*I-digested pBS (pBS-3GFP), and the *Not*I–*Sac*II fragment, which contains the *Saccharomyces cerevisiae ADH1* terminator and the *HIS3MX6* module, was amplified by PCR using pFA6a-GFP (S65T)-HIS3MX6 (Longtine *et al.*, 1998) as a template and inserted into *Not*I- and *Sac*II-digested pBS-3GFP (pBS-3GFP-HIS3). To create an integration plasmid, a fragment of the *SYP1* ORF (nt 2077–2610) was generated by PCR and cloned into the *Bam*HI site of pBS-3GFP-HIS3. To integrate 3GFP at the C-terminus of the *SYP1* gene, the integration plasmid was linearized by *Cla*I and transformed into yeast.

Fluorescence microscopy

Fluorescence microscopy was performed using an Olympus IX81 microscope equipped with a 100×/numerical aperture 1.40 (Olympus, Center Valley, PA) objective and an Orca-AG cooled charge-coupled device camera (Hamamatsu, Hamamatsu, Japan), using MetaMorph software (Universal Imaging, West Chester, PA). Simultaneous imaging of red and green fluorescence was performed using an Olympus IX81 microscope, as described, and an image splitter (Dual-View; Optical Insights, Santa Fe, NM) that divided the red and green components of the images with a 565-nm dichroic mirror and passed the red component through a 630/50-nm filter and the green component through a 530/30-nm filter. Rhodamine–phalloidin staining of filamentous actin and FM4-64 staining were performed as described previously (Toshima *et al.*, 2005).

^{35}S-labeled α-factor internalization assay

Preparation and internalization of ^{35}S-labeled α-factor was performed as described previously (Toshima *et al.*, 2005). Briefly, cells were grown to an OD600 of 0.3 in 50 ml of YPD, briefly centrifuged, and resuspended in 4 ml of YPD containing 1% (wt/vol) bovine serum albumen, 50 mM KH_2PO_4, pH 6.0, and 20 μg/ml uracil, adenine, and histidine. After addition of ^{35}S-labeled α-factor, cell aliquots

Strain	Genotype	Source
JJTY0011	*Mat***a** *his3-Δ200 leu2-3, 112 ura3-52 lys2-801 pan1Δ::PAN1::LEU2*	Toshima lab
JJTY0059	*Mat***a** *his3-Δ200 leu2-3, 112 ura3-52 bar1Δ::LEU2*	Toshima lab
JJTY0147	*Mat***a** *his3-Δ200 leu2-3, 112 ura3-52 lys2-801 pan1Δ::PAN1::LEU2 PAN1-GFP::HIS3*	Toshima lab
JJTY0318	*Matα his3-Δ200 leu2-3, 112 ura3-52 lys2-801 END3-GFP::HIS3*	Toshima lab
JJTY0369	*Mat***a** *his3-Δ200 leu2-3, 112 ura3-52 lys2-801*	Toshima lab
JJTY0393	*Mat***a** *his3-Δ200 leu2-3, 112 ura3-52 SLA1-GFP::KanMX6 ABP1-RFP::HIS3*	Toshima lab
JJTY0943	*Mat***a** *his3-Δ200 leu2-3, 112 ura3-52 pan1Δ::pan1^{EH}::LEU2*	This study
JJTY0950	*Mat***a** *his3-Δ200 leu2-3, 112 ura3-52 pan1Δ::pan1^{EH}::LEU2 PAN1-GFP::HIS3*	This study
JJTY0954	*Matα his3-Δ200 leu2-3, 112 ura3-52 lys2-801 pan1Δ::pan1^{EH}::LEU2 SLA1-GFP::KanMX6 ABP1-mRFP::HIS3*	This study
JJTY0958	*Mat***a** *his3-Δ200 leu2-3, 112 ura3-52 lys2-801 pan1Δ::pan1^{EH}::LEU2 bar1Δ::HIS3*	This study
JJTY0960	*Mat***a** *his3-Δ200 leu2-3, 112 ura3-52 lys2-801 end3Δ::END3::URA3*	This study
JJTY0962	*Mat***a** *his3-Δ200 leu2-3, 112 ura3-52 lys2-801 end3Δ::end3^{EH}::URA3*	This study
JJTY0972	*Mat***a** *his3-Δ200 leu2-3, 112 ura3-52 lys2-801 end3Δ::end3^{EH}::URA3 SLA1-GFP::KanMX6 ABP1-mRFP::HIS3*	This study
JJTY0976	*Mat***a** *his3-Δ200 leu2-3, 112 ura3-52 lys2-801 end3Δ::end3^{EH}::URA3 bar1Δ::LEU2*	This study
JJTY0979	*Mat***a** *his3-Δ200 leu2-3, 112 ura3-52 pan1Δ::pan1^{EH}::LEU2 end3Δ::end3^{EH}::URA3*	This study
JJTY0982	*Matα his3-Δ200 leu2-3, 112 ura3-52 pan1Δ::pan1^{EH}::LEU2 end3Δ::end3^{EH}::URA3 SLA1-GFP::KanMX6 ABP1-mRFP::HIS3*	This study
JJTY0983	*Mat***a** *his3-Δ200 leu2-3, 112 ura3-52 pan1Δ::pan1^{EH}::LEU2 end3Δ::end3^{EH}::URA3 bar1Δ::LEU2*	This study
JJTY1074	*Mat***a** *his3-Δ200 leu2-3, 112 ura3-52 lys2-801 ede1Δ::EDE1::LEU2*	This study
JJTY1075	*Mat***a** *his3-Δ200 leu2-3, 112 ura3-52 lys2-801 ede1Δ::ede1^{EH}::LEU2*	This study
JJTY1077	*Matα his3-Δ200 leu2-3, 112 ura3-52 ede1Δ::ede1^{EH}::LEU2 SLA1-GFP::KanMX6 ABP1-mRFP::HIS3*	This study
JJTY1079	*Mat***a** *his3-Δ200 leu2-3, 112 ura3-52 lys2-801 ede1Δ::ede1^{EH}::LEU2 bar1Δ::HIS3*	This study
JJTY1080	*Matα his3-Δ200 leu2-3, 112 ura3-52 pan1Δ::pan1^{EH}::LEU2 ede1Δ::ede1^{EH}::LEU2 SLA1-GFP::KanMX6 ABP1-mRFP::HIS3*	This study
JJTY1081	*Mat***a** *his3-Δ200 leu2-3, 112 ura3-52 lys2-801 end3Δ::end3^{EH}::URA3 ede1Δ::ede1^{EH}::LEU2 SLA1-GFP::KanMX6 ABP1-mRFP::HIS3*	This study
JJTY1083	*Mat***a** *his3-Δ200 leu2-3, 112 ura3-52 end3Δ::end3^{EH}::URA3 ede1Δ::ede1^{EH}::LEU2*	This study
JJTY1085	*Mat***a** *his3-Δ200 leu2-3, 112 ura3-52 lys2-801 pan1Δ::pan1^{EH}::LEU2 end3Δ::end3^{EH}::URA3 ede1Δ::ede1^{EH}::LEU2*	This study
JJTY1087	*Mat***a** *his3-Δ200 leu2-3, 112 ura3-52 pan1Δ::pan1^{EH}::LEU2 ede1Δ::ede1^{EH}::LEU2*	This study
JJTY1088	*Mat***a** *his3-Δ200 leu2-3, 112 ura3-52 pan1Δ::pan1^{EH}::LEU2 ede1Δ::ede1^{EH}::LEU2 bar1Δ::LEU2*	This study
JJTY1089	*Mat***a** *his3-Δ200 leu2-3, 112 ura3-52 end3Δ::end3^{EH}::URA3 ede1Δ::ede1^{EH}::LEU2 bar1Δ::HIS3*	This study
JJTY1090	*Mat***a** *his3-Δ200 leu2-3, 112 ura3-52 lys2-801 pan1Δ::pan1^{EH}::LEU2 end3Δ::end3^{EH}::URA3 ede1Δ::ede1^{EH}::LEU2 SLA1-GFP::KanMX6 ABP1-mRFP::HIS3*	This study
JJTY1091	*Mat***a** *his3-Δ200 leu2-3, 112 ura3-52 lys2-801 pan1Δ::pan1^{EH}::LEU2 end3Δ::end3^{EH}::URA3 ede1Δ::ede1^{EH}::LEU2 bar1Δ::HIS3*	This study
JJTY1227	*Mat***a** *his3Δ1 leu2Δ0 ura3Δ0 lys2Δ0 YAP1802-GFP::KanMX6*	This study
JJTY1255	*Mat***a** *his3-Δ200 leu2-3, 112 ura3-52 lys2-801 end3Δ::end3^{EH}::URA3 END3-GFP::URA3*	This study
JJTY1256	*Matα his3-Δ200 leu2-3, 112 ura3-52 lys2-801 EDE1-GFP::HIS3*	This study
JJTY1257	*Mat***a** *his3-Δ200 leu2-3, 112 ura3-52 lys2-801 ede1Δ::ede1^{EH}::LEU2 EDE1-GFP::HIS3*	This study
JJTY1258	*Matα his3-Δ200 leu2-3, 112 ura3-52 lys2-801 ENT1-GFP::HIS3*	This study
JJTY1259	*Mat***a** *his3-Δ200 leu2-3, 112 ura3-52 lys2-801 pan1Δ::pan1^{EH}::LEU2 end3Δ::end3^{EH}::URA3 ede1Δ::ede1^{EH}::LEU2 ENT1-GFP::HIS3*	This study

TABLE 1: Yeast strains.

(Continues)

Strain	Genotype	Source
JJTY1262	*Matα his3-Δ200 leu2-3, 112 ura3-52 lys2-801 YAP*Lafer*-GFP::HIS3*	This study
JJTY1263	*Mat***a** *his3-Δ200 leu2-3, 112 ura3-52 lys2-801 pan1Δ::pan1^{EH}::LEU2 end3Δ::end3^{EH}::URA3 ede1Δ::ede1^{EH}::LEU2 YAP1801-GFP::HIS3*	This study
JJTY1928	*Mat***a** *his3-Δ200 leu2-3, 112 ura3-52 lys2-801 SYP1-3GFP::HIS3 ABP1-mRFP::KanMX6*	This study
JJTY1929	*Mat***a** *his3-Δ200 leu2-3, 112 ura3-52 pan1Δ::pan1^{EH}::LEU2 SYP1-3GFP::HIS3 ABP1-mRFP::KanMX6*	This study
JJTY1930	*Mat***a** *his3-Δ200 leu2-3, 112 ura3-52 lys2-801 end3Δ::end3^{EH}::URA3 SYP1-3GFP::HIS3 ABP1-mRFP::KanMX6*	This study
JJTY1931	*Mat***a** *his3-Δ200 leu2-3, 112 ura3-52 lys2-801 ede1Δ::ede1^{EH}::LEU2 SYP1-3GFP::HIS3 ABP1-mRFP::KanMX6*	This study
JJTY1932	*Mat***a** *his3-Δ200 leu2-3, 112 ura3-52 pan1Δ::pan1^{EH}::LEU2 end3Δ::end3^{EH}::URA3 SYP1-3GFP::HIS3 ABP1-mRFP::KanMX6*	This study
JJTY1933	*Mat***a** *his3-Δ200 leu2-3, 112 ura3-52 pan1Δ::pan1^{EH}::LEU2 ede1Δ::ede1^{EH}::LEU2 SYP1-3GFP::HIS3 ABP1-mRFP::KanMX6*	This study
JJTY1934	*Mat***a** *his3-Δ200 leu2-3, 112 ura3-52 end3Δ::end3^{EH}::URA3 ede1Δ::ede1^{EH}::LEU2 SYP1-3GFP::HIS3 ABP1-mRFP::KanMX6*	This study
JJTY1935	*Mat***a** *his3-Δ200 leu2-3, 112 ura3-52 lys2-801 pan1Δ::pan1^{EH}::LEU2 end3Δ::end3^{EH}::URA3 ede1Δ::ede1^{EH}::LEU2 SYP1-3GFP::HIS3 ABP1-mRFP::KanMX6*	This study
JJTY1936	*Matα his3-Δ200 leu2-3, 112 ura3-52 lys2-801 ENT2-GFP::HIS3*	This study
JJTY1937	*Mat***a** *his3-Δ200 leu2-3, 112 ura3-52 lys2-801 pan1Δ::pan1^{EH}::LEU2 end3Δ::end3^{EH}::URA3 ede1Δ::ede1^{EH}::LEU2 ENT2-GFP::HIS3*	This study
JJTY1938	*Matα his3-Δ200 leu2-3, 112 ura3-52 lys2-801 SLA2-GFP::HIS3*	This study
JJTY1939	*Mat***a** *his3-Δ200 leu2-3, 112 ura3-52 lys2-801 pan1Δ::pan1^{EH}::LEU2 end3Δ::end3^{EH}::URA3 ede1Δ::ede1^{EH}::LEU2 SLA2-GFP::HIS3*	This study
JJTY1940	*Mat***a** *his3-Δ200 leu2-3, 112 ura3-52 lys2-801 pan1Δ::pan1^{EH}::LEU2 end3Δ::end3^{EH}::URA3 ede1Δ::ede1^{EH}::LEU2 YAP1802-GFP::HIS3*	This study
JJTY2421	*Mat***a** *his3-Δ200 leu2-3, 112 ura3-52 lys2-801 SYP1-3GFP::HIS3 Sla1-mCherry::KanMX*	This study
JJTY2422	*Mat***a** *his3-Δ200 leu2-3, 112 ura3-52 lys2-801 pan1Δ::pan1^{EH}::LEU2 Syp1-3GFP::HIS3 Sla1-mCherry::KanMX*	This study
JJTY2423	*Mat***a** *his3-Δ200 leu2-3, 112 ura3-52 lys2-801 end3Δ::end3^{EH}::URA3 Syp1-3GFP::HIS3 Sla1-mCherry::KanMX*	This study
JJTY2424	*Mat***a** *his3-Δ200 leu2-3, 112 ura3-52 lys2-801 ede1Δ::ede1^{EH}::LEU2 Syp1-3GFP::HIS3 Sla1-mCherry:: KanMX*	This study
JJTY2426	*Mat***a** *his3-Δ200 leu2-3, 112 ura3-52 pan1Δ::pan1^{EH}::LEU2 END3-GFP::HIS3*	This study
JJTY2427	*Mat***a** *his3-Δ200 leu2-3, 112 ura3-52 pan1Δ::pan1^{EH}::LEU EDE1-GFP::HIS3*	This study
JJTY2428	*Mat***a** *his3-Δ200 leu2-3, 112 ura3-52 lys2-801 ede1Δ::ede1^{EH}::LEU2 PAN1- GFP::HIS3*	This study
JJTY2429	*Mat***a** *his3-Δ200 leu2-3, 112 ura3-52 ede1Δ::ede1^{EH}::LEU2 END3-GFP::HIS3*	This study
JJTY2430	*Mat***a** *his3-Δ200 leu2-3, 112 ura3-52 lys2-801 end3Δ::end3^{EH}::URA3 PAN1-GFP::HIS3*	This study
JJTY2431	*Mat***a** *his3-Δ200 leu2-3, 112 ura3-52 lys2-801 end3Δ::end3^{EH}::URA3 EDE1-GFP::HIS3*	This study
JJTY2432	*Mat***a** *his3-Δ200 leu2-3, 112 ura3-52 pan1Δ::pan1^{EH}::LEU2 end3Δ::end3^{EH}::URA3 EDE1-GFP::HIS3*	This study
JJTY2433	*Mat***a** *his3-Δ200 leu2-3, 112 ura3-52 pan1Δ::pan1^{EH}::LEU2 ede1Δ::ede1^{EH}::LEU2 END3-GFP::HIS3*	This study
JJTY2434	*Mat***a** *his3-Δ200 leu2-3, 112 ura3-52 end3Δ::end3^{EH}::URA3 ede1Δ::ede1^{EH}::LEU2 PAN1-GFP*	This study

TABLE 1: Yeast strains. (Continued)

were withdrawn at various time points and subjected to a wash in pH 1 buffer to remove surface-bound α-factor so internal α-factor could be measured or in pH 6 buffer to determine the total (internal and bound) α-factor. The amount of cell-associated radioactivity after each wash was determined by scintillation counting. Each experiment was performed at least three times.

ACKNOWLEDGMENTS

We thank R. Kashikuma, E. Furuya, and M. Saito for construction of plasmids and strains. We also thank the members of the Toshima lab for sharing materials and for helpful discussions. This work was supported by Japan Society for the Promotion of Science (to J.Y.T.) and the Novartis Foundation (Japan), the Mitsubishi Foundation, the Naito Foundation, the Mochida Memorial Foundation for Medical and Pharmaceutical Research, the Futaba Electronics Memorial Foundation, the Astellas Foundation for Research on Metabolic Disorders, the Hamaguchi Foundation for the Advancement of Biochemistry, the Takeda Science Foundation, and the Kurata Memorial Hitachi Science and Technology Foundation (to J.T.).

REFERENCES

Aguilar RC, Watson HA, Wendland B (2003). The yeast epsin Ent1 is recruited to membranes through multiple independent interactions. J Biol Chem 278, 10737–10743.

Ahle S, Ungewickell E (1986). Purification and properties of a new clathrin assembly protein. EMBO J 5, 3143–3149.

Benedetti H, Raths S, Crausaz F, Riezman H (1994). The END3 gene encodes a protein that is required for the internalization step of endocytosis and for actin cytoskeleton organization in yeast. Mol Biol Cell 5, 1023–1037.

Benmerah A, Bayrou M, Cerf-Bensussan N, Dautry-Varsat A (1999). Inhibition of clathrin-coated pit assembly by an Eps15 mutant. J Cell Sci 112, 1303–1311.

Benmerah A, Begue B, Dautry-Varsat A, Cerf-Bensussan N (1996). The ear of alpha-adaptin interacts with the COOH-terminal domain of the Eps 15 protein. J Biol Chem 271, 12111–12116.

Benmerah A, Gagnon J, Begue B, Megarbane B, Dautry-Varsat A, Cerf-Bensussan N (1995). The tyrosine kinase substrate eps15 is constitutively associated with the plasma membrane adaptor AP-2. J Cell Biol 131, 1831–1838.

Benmerah A, Poupon V, Cerf-Bensussan N, Dautry-Varsat A (2000). Mapping of Eps15 domains involved in its targeting to clathrin-coated pits. J Biol Chem 275, 3288–3295.

Chen H, Fre S, Slepnev VI, Capua MR, Takei K, Butler MH, Di Fiore PP, De Camilli P (1998). Epsin is an EH-domain-binding protein implicated in clathrin-mediated endocytosis. Nature 394, 793–797.

de Beer T, Carter RE, Lobel-Rice KE, Sorkin A, Overduin M (1998). Structure and Asn-Pro-Phe binding pocket of the Eps15 homology domain. Science 281, 1357–1360.

de Beer T, Hoofnagle AN, Enmon JL, Bowers RC, Yamabhai M, Kay BK, Overduin M (2000). Molecular mechanism of NPF recognition by EH domains. Nat Struct Biol 7, 1018–1022.

Di Fiore PP, Pelicci PG, Sorkin A (1997). EH: a novel protein-protein interaction domain potentially involved in intracellular sorting. Trends Biochem Sci 22, 411–413.

Ehrlich M, Boll W, Van Oijen A, Hariharan R, Chandran K, Nibert ML, Kirchhausen T (2004). Endocytosis by random initiation and stabilization of clathrin-coated pits. Cell 118, 591–605.

Engqvist-Goldstein AE, Drubin DG (2003). Actin assembly and endocytosis: from yeast to mammals. Annu Rev Cell Dev Biol 19, 287–332.

Geli MI, Riezman H (1998). Endocytic internalization in yeast and animal cells: similar and different. J Cell Sci 111, 1031–1037.

Grant BD, Caplan S (2008). Mechanisms of EHD/RME-1 protein function in endocytic transport. Traffic 9, 2043–2052.

Howard JP, Hutton JL, Olson JM, Payne GS (2002). Sla1p serves as the targeting signal recognition factor for NPFX(1,2)D-mediated endocytosis. J Cell Biol 157, 315–326.

Huang KM, D'Hondt K, Riezman H, Lemmon SK (1999). Clathrin functions in the absence of heterotetrameric adaptors and AP180-related proteins in yeast. EMBO J 18, 3897–3908.

Kaksonen M, Sun Y, Drubin DG (2003). A pathway for association of receptors, adaptors, and actin during endocytic internalization. Cell 115, 475–487.

Kaksonen M, Toret CP, Drubin DG (2005). A modular design for the clathrin- and actin-mediated endocytosis machinery. Cell 123, 305–320.

Longtine MS, McKenzie A 3rd, Demarini DJ, Shah NG, Wach A, Brachat A, Philippsen P, Pringle JR (1998). Additional modules for versatile and economical PCR-based gene deletion and modification in *Saccharomyces cerevisiae*. Yeast 14, 953–961.

Maldonado-Baez L, Dores MR, Perkins EM, Drivas TG, Hicke L, Wendland B (2008). Interaction between Epsin/Yap180 adaptors and the scaffolds Ede1/Pan1 is required for endocytosis. Mol Biol Cell 19, 2936–2948.

Merrifield CJ, Feldman ME, Wan L, Almers W (2002). Imaging actin and dynamin recruitment during invagination of single clathrin-coated pits. Nat Cell Biol 4, 691–698.

Mettlen M, Stoeber M, Loerke D, Antonescu CN, Danuser G, Schmid SL (2009). Endocytic accessory proteins are functionally distinguished by their differential effects on the maturation of clathrin-coated pits. Mol Biol Cell 20, 3251–3260.

Meyerholz A, Hinrichsen L, Groos S, Esk PC, Brandes G, Ungewickell EJ (2005). Effect of clathrin assembly lymphoid myeloid leukemia protein depletion on clathrin coat formation. Traffic 6, 1225–1234.

Miliaras NB, Wendland B (2004). EH proteins: multivalent regulators of endocytosis (and other pathways). Cell Biochem Biophys 41, 295–318.

Morgan JR, Prasad K, Jin S, Augustine GJ, Lafer EM (2003). Eps15 homology domain-NPF motif interactions regulate clathrin coat assembly during synaptic vesicle recycling. J Biol Chem 278, 33583–33592.

Morgan JR, Zhao X, Womack M, Prasad K, Augustine GJ, Lafer EM (1999). A role for the clathrin assembly domain of AP180 in synaptic vesicle endocytosis. J Neurosci 19, 10201–10212.

Naslavsky N, Rahajeng J, Chenavas S, Sorgen PL, Caplan S (2007). EHD1 and Eps15 interact with phosphatidylinositols via their Eps15 homology domains. J Biol Chem 282, 16612–16622.

Newpher TM, Lemmon SK (2006). Clathrin is important for normal actin dynamics and progression of Sla2p-containing patches during endocytosis in yeast. Traffic 7, 574–588.

Newpher TM, Smith RP, Lemmon V, Lemmon SK (2005). In vivo dynamics of clathrin and its adaptor-dependent recruitment to the actin-based endocytic machinery in yeast. Dev Cell 9, 87–98.

Paoluzi S, Castagnoli L, Lauro I, Salcini AE, Coda L, Fre S, Confalonieri S, Pelicci PG, Di Fiore PP, Cesareni G (1998). Recognition specificity of individual EH domains of mammals and yeast. EMBO J 17, 6541–6550.

Raths S, Rohrer J, Crausaz F, Riezman H (1993). end3 and end4: two mutants defective in receptor-mediated and fluid-phase endocytosis in *Saccharomyces cerevisiae*. J Cell Biol 120, 55–65.

Reider A, Barker SL, Mishra SK, Im YJ, Maldonado-Baez L, Hurley JH, Traub LM, Wendland B (2009). Syp1 is a conserved endocytic adaptor that contains domains involved in cargo selection and membrane tubulation. EMBO J 28, 3103–3116.

Salcini AE, Confalonieri S, Doria M, Santolini E, Tassi E, Minenkova O, Cesareni G, Pelicci PG, Di Fiore PP (1997). Binding specificity and in vivo targets of the EH domain, a novel protein-protein interaction module. Genes Dev 11, 2239–2249.

Santolini E, Salcini AE, Kay BK, Yamabhai M, Di Fiore PP (1999). The EH network. Exp Cell Res 253, 186–209.

Sorkin A (2004). Cargo recognition during clathrin-mediated endocytosis: a team effort. Curr Opin Cell Biol 16, 392–399.

Stimpson HE, Toret CP, Cheng AT, Pauly BS, Drubin DG (2009). Early-arriving Syp1p and Ede1p function in endocytic site placement and formation in budding yeast. Mol Biol Cell 20, 4640–4651.

Sun Y, Martin AC, Drubin DG (2006). Endocytic internalization in budding yeast requires coordinated actin nucleation and myosin motor activity. Dev Cell 11, 33–46.

Tang HY, Cai M (1996). The EH-domain-containing protein Pan1 is required for normal organization of the actin cytoskeleton in *Saccharomyces cerevisiae*. Mol Cell Biol 16, 4897–4914.

Tang HY, Munn A, Cai M (1997). EH domain proteins Pan1p and End3p are components of a complex that plays a dual role in organization of the cortical actin cytoskeleton and endocytosis in *Saccharomyces cerevisiae*. Mol Cell Biol 17, 4294–4304.

Tang HY, Xu J, Cai M (2000). Pan1p, End3p, and S1a1p, three yeast proteins required for normal cortical actin cytoskeleton organization, associate with each other and play essential roles in cell wall morphogenesis. Mol Cell Biol 20, 12–25.

Tonikian R *et al.* (2009). Bayesian modeling of the yeast SH3 domain interactome predicts spatiotemporal dynamics of endocytosis proteins. PLoS Biol 7, e1000218.

Toret CP, Drubin DG (2006). The budding yeast endocytic pathway. J Cell Sci 119, 4585–4587.

Toshima J, Toshima JY, Duncan MC, Cope MJ, Sun Y, Martin AC, Anderson S, Yates JR 3rd, Mizuno K, Drubin DG (2007). Negative regulation of yeast Eps15-like Arp2/3 complex activator, Pan1p, by the Hip1R-related protein, Sla2p, during endocytosis. Mol Biol Cell 18, 658–668.

Toshima J, Toshima JY, Martin AC, Drubin DG (2005). Phosphoregulation of Arp2/3-dependent actin assembly during receptor-mediated endocytosis. Nat Cell Biol 7, 246–254.
Toshima JY, Toshima J, Kaksonen M, Martin AC, King DS, Drubin DG (2006). Spatial dynamics of receptor-mediated endocytic trafficking in budding yeast revealed by using fluorescent alpha-factor derivatives. Proc Natl Acad Sci USA 103, 5793–5798.
van Delft S, Schumacher C, Hage W, Verkleij AJ, van Bergen en Henegouwen PM (1997). Association and colocalization of Eps15 with adaptor protein-2 and clathrin. J Cell Biol 136, 811–821.
Wendland B, Emr SD (1998). Pan1p, yeast eps15, functions as a multivalent adaptor that coordinates protein-protein interactions essential for endocytosis. J Cell Biol 141, 71–84.
Wendland B, McCaffery JM, Xiao Q, Emr SD (1996). A novel fluorescence-activated cell sorter-based screen for yeast endocytosis mutants identifies a yeast homologue of mammalian eps15. J Cell Biol 135, 1485–1500.
Wendland B, Steece KE, Emr SD (1999). Yeast epsins contain an essential N-terminal ENTH domain, bind clathrin and are required for endocytosis. EMBO J 18, 4383–4393.
Ye W, Ali N, Bembenek ME, Shears SB, Lafer EM (1995). Inhibition of clathrin assembly by high affinity binding of specific inositol polyphosphates to the synapse-specific clathrin assembly protein AP-3. J Biol Chem 270, 1564–1568.
Ye W, Lafer EM (1995). Bacterially expressed F1-20/AP-3 assembles clathrin into cages with a narrow size distribution: implications for the regulation of quantal size during neurotransmission. J Neurosci Res 41, 15–26.